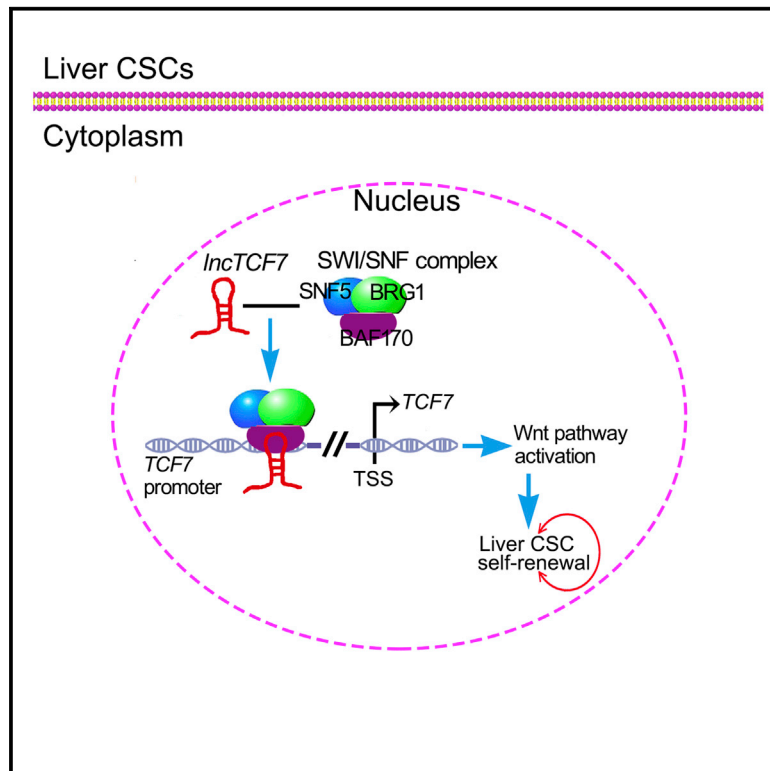# Cell Stem Cell

The Long Noncoding RNA *lncTCF7* Promotes Self-Renewal of Human Liver Cancer Stem Cells through Activation of Wnt Signaling

Graphical Abstract

Authors

Yanying Wang, Lei He, ..., Runsheng Chen, Zusen Fan

Correspondence

crs@sun5.ibp.ac.cn (R.C.), fanz@moon.ibp.ac.cn (Z.F.)

In Brief

Wang et al. have identified a long noncoding RNA, *lncTCF7*, that activates Wnt signaling to promote liver cancer stem cell self-renewal and tumor propagation. Targeting this pathway could help address the high recurrence and heterogeneity of liver cancer.

Highlights

- The long noncoding RNA *lncTCF7* is highly expressed in liver cancer tissues and CSCs

- *LncTCF7* is important for self-renewal of liver CSCs

- *LncTCF7* activates the Wnt signaling pathway through TCF7 expression

- *LncTCF7* recruits the SWI/SNF complex to activate the *TCF7* promoter

Accession Numbers

GSE66515
GSE66529

CellPress

Cell Press

The Long Noncoding RNA *lncTCF7* Promotes Self-Renewal of Human Liver Cancer Stem Cells through Activation of Wnt Signaling

Yanying Wang,[1,5] Lei He,[2,5] Ying Du,[1] Pingping Zhu,[1] Guanling Huang,[1,3] Jianjun Luo,[4] Xinlong Yan,[1] Buqing Ye,[1] Chong Li,[1] Pengyan Xia,[1] Geng Zhang,[1] Yong Tian,[4] Runsheng Chen,[4,*] and Zusen Fan[1,3,*]

[1]CAS Key Laboratory of Infection and Immunity, Institute of Biophysics, Chinese Academy of Sciences, Beijing 100101, China
[2]Department of Hepatobiliary Surgery, PLA General Hospital, Beijing 100853, China
[3]University of Chinese Academy of Sciences, Beijing 100049, China
[4]CAS Key Laboratory of RNA Biology, Institute of Biophysics, Chinese Academy of Sciences, Beijing 100101, China
[5]Co-first author
*Correspondence: crs@sun5.ibp.ac.cn (R.C.), fanz@moon.ibp.ac.cn (Z.F.)
http://dx.doi.org/10.1016/j.stem.2015.03.003

SUMMARY

Hepatocellular carcinoma (HCC) is the most prevalent subtype of liver cancer, and it is characterized by a high rate of recurrence and heterogeneity. Liver cancer stem cells (CSCs) may well contribute to both of these pathological properties, but the mechanisms underlying their self-renewal and maintenance are poorly understood. Here, using transcriptome microarray analysis, we identified a long noncoding RNA (lncRNA) termed *lncTCF7* that is highly expressed in HCC tumors and liver CSCs. *LncTCF7* is required for liver CSC self-renewal and tumor propagation. Mechanistically, *lncTCF7* recruits the SWI/SNF complex to the promoter of *TCF7* to regulate its expression, leading to activation of Wnt signaling. Our data suggest that *lncTCF7*-mediated Wnt signaling primes liver CSC self-renewal and tumor propagation. In sum, therefore, we have identified an lncRNA-based Wnt signaling regulatory circuit that promotes tumorigenic activity in liver cancer stem cells, highlighting the role that lncRNAs can play in tumor growth and propagation.

INTRODUCTION

Liver cancer is the fifth most commonly diagnosed cancer and the second most frequent cause of cancer death in men worldwide (Jemal et al., 2011). Hepatocellular carcinoma (HCC) represents the major histological subtype, accounting for ∼70%–85% of cases of primary liver cancer. Unfortunately, the 5-year survival rate of HCC subjects remains poor, and more than 750,000 HCC subjects die each year. Although previous studies identified many aberrantly expressed protein-coding genes in HCC, novel molecular markers that can help in early diagnosis and risk assessment are still urgently needed (Ji et al., 2009; Yamashita and Wang, 2013). New therapeutic approaches are likely to derive from an improved understanding of the molecular basis of HCC.

The high rate of recurrence and heterogeneity are the two major features of HCC (Visvader, 2011). Recent studies have suggested that heterogeneity is a result of the hierarchical organization of tumor cells by a subset of cells with stem/progenitor cell features known as cancer stem cells (CSCs) (Easwaran et al., 2014). These CSCs within tumor bulk display the capacity to self-renew, differentiate, and give rise to a new tumor (Visvader and Lindeman, 2012), accounting for a hierarchical organization of heterogeneous cancer cells and a high rate of cancerous recurrence. Liver CSCs can be enriched with several defined surface markers, including epithelial cell adhesion molecule (EpCAM), CD133, CD13, CD90, CD44, CD24, and calcium channel $\alpha 2\delta 1$ subunit, among others (Haraguchi et al., 2010; Lee et al., 2011; Ma et al., 2007; Zhao et al., 2013). However, how liver CSCs sustain their self-renewal remains largely unknown.

Long noncoding RNAs (lncRNAs) are defined as transcripts longer than 200 nucleotides (nt) that are 5′ capped and 3′ polyadenylated, yet this class of transcripts has limited coding potential. LncRNAs function in a wide range of biological processes and can regulate gene expression in *cis* or in *trans* by diverse mechanisms (Batista and Chang, 2013; Cech and Steitz, 2014; Ulitsky and Bartel, 2013). LncRNA-mediated biology has been implicated in many cellular processes (Ulitsky and Bartel, 2013). In cancer, lncRNAs have been reported to act as a prominent layer of transcriptional regulation, often by collaborating with chromatin remodeling complexes (Gupta et al., 2010; Prensner et al., 2013; Yang et al., 2013; Yuan et al., 2014). The SWI/SNF complex is an evolutionarily conserved multisubunit complex that mobilizes nucleosomes and remodels chromatin using the energy of ATP hydrolysis (Helming et al., 2014; Wilson and Roberts, 2011). The SWI/SNF complex associates with transcription factors, coactivators, or coexpressors to regulate gene expression (Tolstorukov et al., 2013; You et al., 2013). Inactivating mutations in several SWI/SNF subunits have been identified in various human cancers (Jones et al., 2010; Kadoch et al., 2013; Li et al., 2011), suggesting that mutations of some individual subunits promote tumorigenesis. Additionally, the SWI/SNF complex has been implicated in being involved in controlling mammalian stem cell self-renewal and differentiation (Eroglu et al., 2014; Yu et al., 2013; Zeng et al., 2013). However, how the SWI/SNF complex functions in CSCs remains elusive. In

CrossMark

this study, we found that *lncTCF7* is required for the self-renewal maintenance of liver CSCs. *LncTCF7* recruits the SWI/SNF complex to trigger TCF7 expression, leading to activation of Wnt signaling for priming liver CSC self-renewal.

RESULTS

LncTCF7 Is Highly Expressed in Liver CSCs

Although CD13 (Haraguchi et al., 2010) and CD133 (Ma et al., 2007) have been widely used as liver CSC surface markers, CD133 or CD13 alone could enrich more cell populations in HCC cell lines or HCC primary samples (Figures S1A and S1B). Haraguchi et al. (2010) demonstrated that the CD13$^+$CD133$^+$ cell fraction exhibited slow growth compared with their counterpart CD13$^-$CD133$^-$ cells. Moreover, the CD13$^+$CD133$^+$ cell fraction was highly resistant to chemical drug treatments compared with their CD13$^-$CD133$^-$ subset. Notably, we observed that the CD13$^+$CD133$^+$ cell subsets were successfully enriched in seven cell lines out of nine HCC cell lines we tested and in over 90% of 30 HCC primary samples we examined (Figure S1B). Thus, we combined CD13 and CD133 to enrich the CD13$^+$CD133$^+$ cell fraction and thereby identify them as hepatic CSCs in this study.

We then sorted CD13$^+$CD133$^+$ cells, presumptively liver CSCs, from Hep3B, Huh7, and PLC/PRF/5 HCC cell lines. Actually, the CD13$^+$CD133$^+$ subset derived from Hep3B cells significantly enhanced oncosphere formation compared to CD13$^-$CD133$^-$ cells (10.3% ± 1.3% versus 2.6% ± 0.3%; p = 0.003) (Figure S1C). In addition, the tumor sphere formation frequencies of CD13$^+$CD133$^+$ and CD13$^+$CD133$^-$ subsets of Hep3B cells were 10.3% ± 1.3% versus 6.1% ± 1.1% (p = 0.0253); CD13$^+$CD133$^+$ versus CD13$^-$CD133$^+$ fractions of Hep3B cells were 10.3% ± 1.3% to 5.2% ± 1.3% (p = 0.0226) (Figure S1C). Similar observations were obtained using Huh7 and PLC/PRF/5 cells (Figure S1C). Consistently, the tumor-initiating ability of the CD13$^+$CD133$^+$ subset derived from Hep3B cells was significantly higher than that of CD13$^+$ or CD133$^+$ cells alone (Figures S1D and S1E). Similar results were achieved with Huh7 cells. We concluded that the tumorigenic capacity of CD13$^+$CD133$^+$ cells was much higher than that of CD13$^+$ or CD133$^+$ cells alone. Of note, there was no significant difference in the proliferative capacity between CD13$^+$CD133$^+$ cells and CD13$^-$CD133$^-$ cells through cell-cycle analysis (Figure S1F). To identify lncRNAs involved in liver CSCs, we conducted transcriptome microarray analysis of CD13$^+$CD133$^+$ cells (hereafter called liver CSCs) and CD13$^-$CD133$^-$ cells (hereafter referred to as non-CSCs) sorted from the three above mentioned HCC cell lines. 286 noncoding RNA transcripts were aberrantly expressed in liver CSCs compared with non-CSCs (Figure 1A), with some of those differential lncRNAs validated in liver CSCs when we detected ten randomly selected lncRNAs (Figure S1G).

Since lncRNAs can act in *cis* to regulate expression of neighboring genes or in *trans* by diverse mechanisms (Rinn and Chang, 2012), we concentrated on intergenic lncRNAs, which were highly expressed in liver CSCs and located in the nearby stem transcription factors and coding genes related to stem signaling pathways. Among these highly expressed intergenic lncRNAs, we focused on an uncharacterized lncRNA, termed *lncTCF7* (gene symbol TCONS_00009511-XLOC_004555). *LncTCF7* is one of the most highly expressed lncRNAs in liver CSCs (Figure 1A and Figure S1G), residing on chromosome 5 in humans between the heat shock 70 kDa protein 4 (*HSPA4*) and T cell factor 7 (*TCF7*) genes (Figure 1B). *LncTCF7* was composed of three exons and spanned nearly 3.6 kilobases (kb), identifying it as a modestly conserved locus. We further confirmed that *lncTCF7* was highly expressed in liver CSCs (Figure 1C), as well as in oncosphere cells derived from HCC cell lines and HCC primary samples (Figures 1D and 1E). We next examined a cohort of 37 paired HCC tumor and peri-tumor tissues, along with 14 hepatitis B virus (HBV)-infected liver cirrhotic tissues and 8 normal liver tissues (Table S1). We observed that *lncTCF7* was significantly highly expressed in HCC tumors (Figure 1F and Figure S1H) and HCC cell lines (Figure S1I), whereas it was almost undetectable in liver cirrhosis samples and healthy liver tissues (Figure 1F and Figure S1H). In addition, *lncTCF7* was not detectable in some other normal primary tissues we examined (Figure S1J), suggesting a more restricted fashion of *lncTCF7* expression.

We further examined the transcripts of *lncTCF7* in liver CSCs by northern blot. Only one transcript variant of *lncTCF7* was in liver CSCs, with a length between 500 to 1,000 bases (Figure 1G). However, *lncTCF7* expression was much lower in non-CSCs. A total length of 683 nt of *lncTCF7* transcript was determined by a rapid amplification of cDNA ends (RACE) assay (Figure S1K), which displayed no coding potentiality (Figures S1L and S1M). Furthermore, *lncTCF7* was localized in the nuclei of HCC tumor cells through RNA fluorescence in situ hybridization (RNA-FISH) and cellular fractionation assays (Figures 1H and 1I). *LncTCF7* was highly expressed in oncosphere cells, but it was poorly expressed in non-sphere tumor cells. These data indicate that *lncTCF7*, as an lncRNA, was highly expressed in HCC tumor tissues and liver CSCs.

LncTCF7 Is Required for Self-Renewal Maintenance of Liver CSCs

To determine the role of *lncTCF7* in liver CSC self-renewal, we silenced *lncTCF7* against either exon 1 or 3 in liver CSCs using lentivirus-mediated short hairpins RNAs (shRNAs) (Figure 2A). shRNA-2 (against exon 3) achieved more effective knockdown efficiency. Notably, *lncTCF7* depletion significantly reduced the expression of pluripotent transcription factors Sox2, Nanog, and Oct4 compared with scrambled control (shCtrl) cells (Figure 2B). By contrast, *lncTCF7* knockdown did not affect *c-Myc* expression. Actually, *c-Myc* was highly expressed in both *lncTCF7* silenced and shCtrl liver CSCs, whose expression was not significantly altered in loss-of-function experiments (Figure 2B). Additionally, *lncTCF7* knockdown remarkably impaired generation of the fraction of CD13$^+$CD133$^+$ cells (CSCs) (Figure 2C). Importantly, *lncTCF7* depletion dramatically reduced primary (1st), secondary (2nd), and tertiary (3rd) oncosphere formation of HCC cell lines and HCC primary cells (Figure 2D).

Consistently, *lncTCF7* silencing also impaired 2nd and 3rd oncosphere formation derived from their primary oncosphere cells. Similar observations were obtained in *lncTCF7* silenced PLC/PRF/5 cells (data not shown). Consequently, *lncTCF7* depletion in HCC primary tumor cells significantly reduced the expression of *Sox2* and *Nanog* (Figure 2E). More importantly, we conducted 2nd and 3rd generation xenograft tumor growth for the CD13$^+$CD133$^+$ cell subsets derived from HCC cell lines and primary samples. We noticed that CD13$^+$CD133$^+$ cell populations
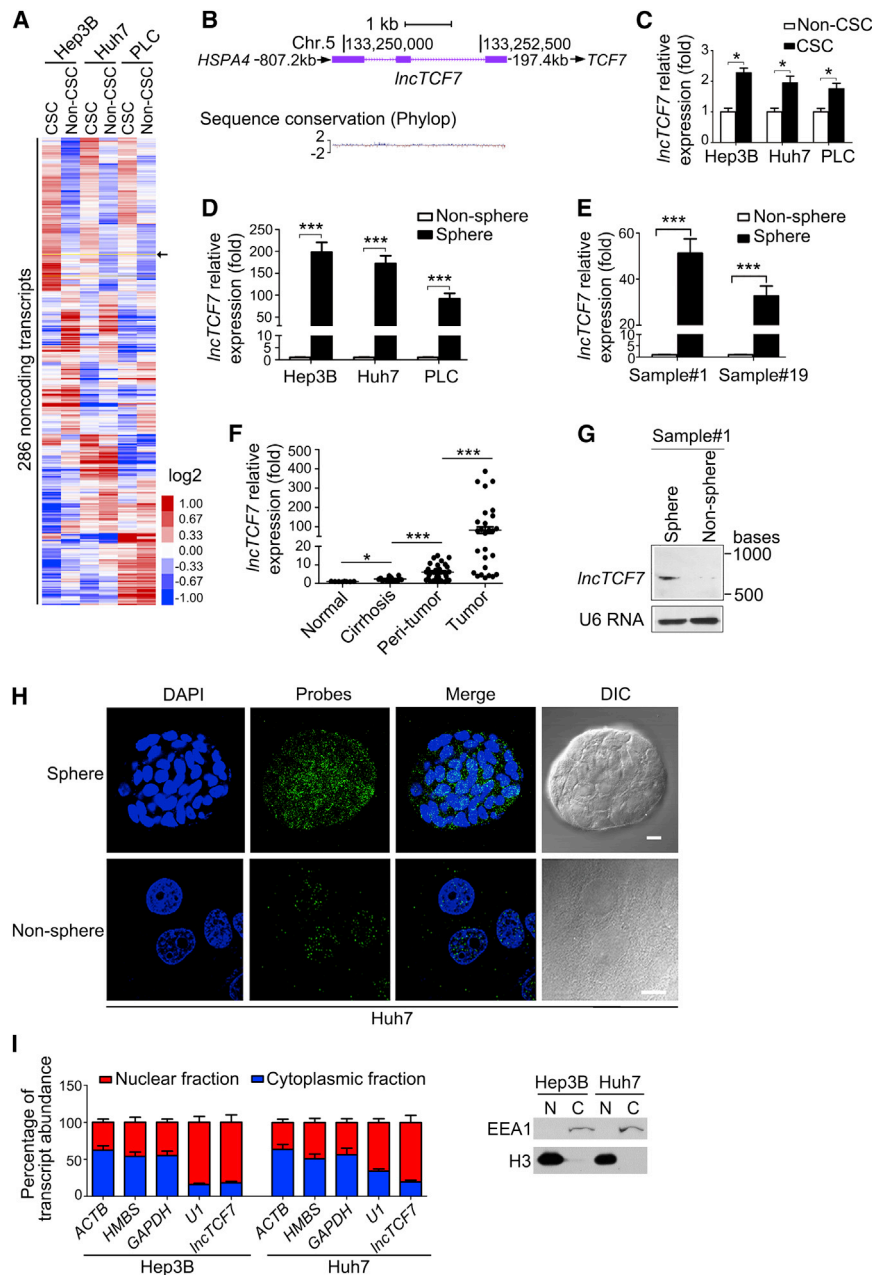
Figure 1. LncTCF7 Is Highly Expressed in Liver CSCs

(A) Geometric mean-centered, hierarchical cluster heat map from microarray data. 286 annotated noncoding RNAs (p < 0.05) were represented in liver CSC (CD13$^+$CD133$^+$) compared with non-CSC (CD13$^-$CD133$^-$) cells sorted from HCC cell lines, Hep3B, Huh7, and PLC/PRF/5 (PLC). Black arrowhead denotes lncTCF7.

(B) Schematic annotation of lncTCF7 genomic locus on chromosome 5. Blue rectangles represent exons (upper panel). Sequence conservation was analyzed by Phylop software (lower panel).

(C) LncTCF7 was detected in liver CSCs and non-CSCs sorted from HCC cell lines by quantitative real-time PCR analysis. Relative gene expression values were normalized to endogenous 18S rRNA unless noted otherwise in this study. Results are shown as means ± SD.

(D and E) LncTCF7 was analyzed in oncosphere and non-oncosphere cells derived from three HCC cell lines and HCC primary cells. Results are shown as means ± SD.

(F) LncTCF7 was detected in HCC tumor tissues paired with adjacent tumor tissues (n = 37), liver cirrhosis tissues (n = 14), and normal liver tissues (n = 8). Data were normalized to endogenous 18S rRNA expression and normal liver tissues were assigned a value of 1.

(G) A 363 nt probe of lncTCF7 was labeled for northern blot analysis. RNAs were extracted from sphere and non-sphere cells derived from HCC primary specimens. U6 RNA was used as a loading control.

(H) LncTCF7 intracellular localization was visualized in HCC oncosphere and non-sphere cells by RNA-FISH assays. Representative images of lncTCF7 in Huh7 oncosphere (Sphere) and non-oncosphere cells (Non-sphere) are shown. DAPI, 4',6-diamidino-2-phenylindole. Probes, lncTCF7. Scale bar, 10 μm.

(I) Fractionation of HCC oncosphere cells followed by quantitative real-time PCR (left panel) and fractionation controls by immnoblotting (right panel). U1 RNA served as a positive control for nuclear gene expression. EEA1, endosome antigen 1; N, Nuclear fraction; C, Cytoplasmic fraction. Data are shown as means ± SD. *p < 0.05, **p < 0.01, and ***p < 0.001 by two-tailed Student's t test. Data are representative of at least three independent experiments. See also Figure S1 and Table S1.

were still enriched from the 2nd and 3rd generation xenograft tumors (data not shown). The CD13$^+$CD133$^+$ cell populations from the 2nd and 3rd generation displayed stronger tumor-initiating capacities (Figure S2A) and oncosphere forming abilities (Figure S2B), indicating a long-term self-renewal capacity of the CD13$^+$CD133$^+$ cell population. Moreover, Ki67 signals were not apparently altered in liver CSCs compared with non-CSCs (Figure S2C). However, the amount of Sox2 was significantly increased in liver CSCs, but not in non-CSCs. By contrast, lncTCF7 overexpression remarkably enhanced Sox2 signals in liver CSCs, whereas Ki67 was not altered in lncTCF7-overexpressing CSCs compared to empty-vector-treated cells (Figure S2D). Similar observations were obtained in xenograft tumors (Figure S2E), suggesting lncTCF7-mediated tumorigenicity in liver cancer is mainly caused by the self-renewal capacity of CSCs.

We next explored the role of lncTCF7 in tumor-initiating formation. We performed subcutaneous injection of BALB/c nude mice with stable knockdown of lncTCF7 and shCtrl cells. LncTCF7 depletion resulted in a much weaker tumor presence compared with shCtrl primary tumor cells as assessed by a limiting dilution xenograft analysis (Figure 2F), suggesting that lncTCF7 knockdown reduced tumor initiating capacity. Moreover, lncTCF7 depletion significantly suppressed xenograft
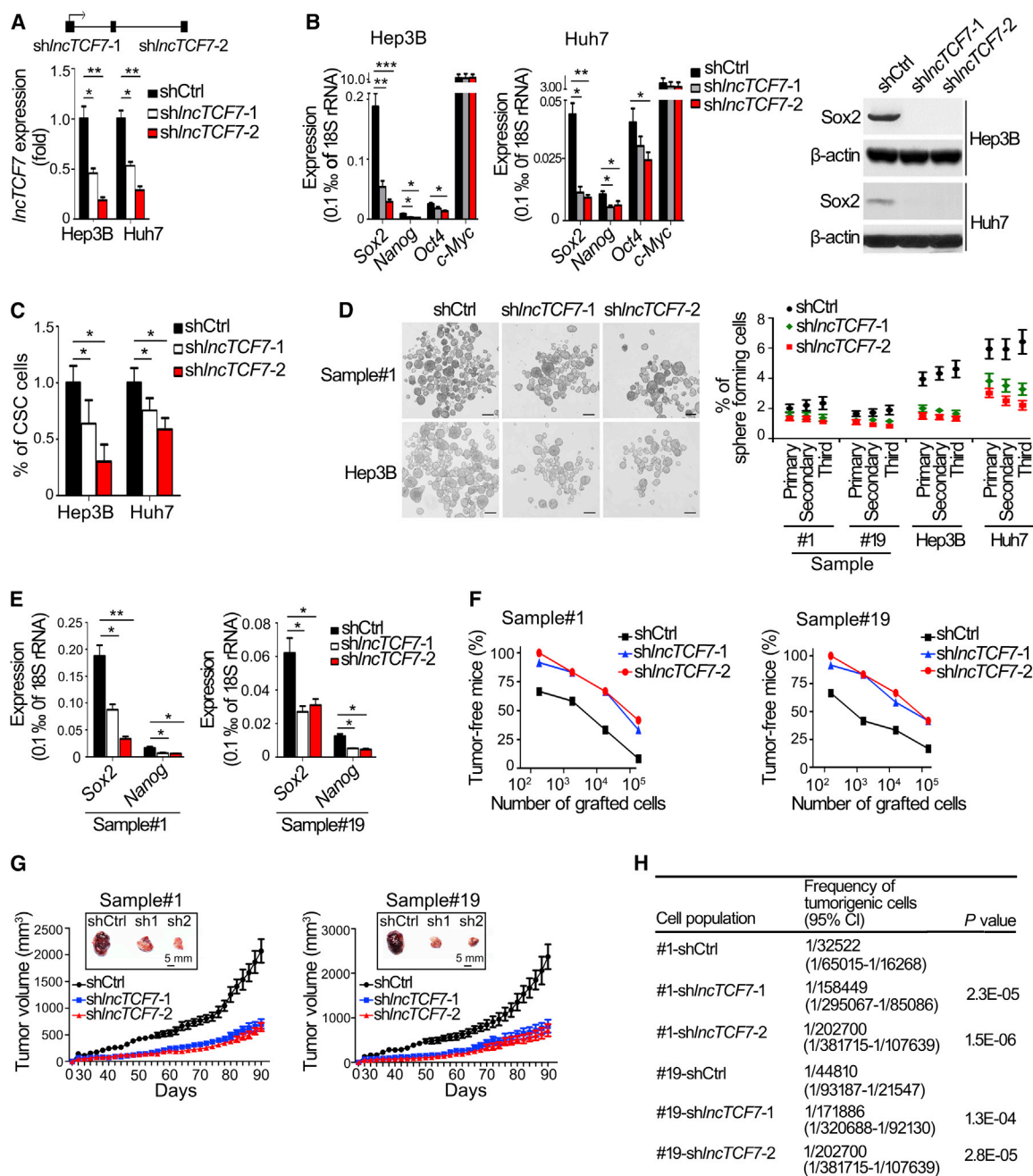
Figure 2. LncTCF7 Is Required for the Self-Renewal Maintenance of Liver CSCs

(A) LncTCF7 was silenced in liver CSCs by two independent shRNAs targeting either exon 1 or 3. LncTCF7-silenced stable cell lines were established. Data are shown as means ± SD.

(B) Pluripotent transcription factors were analyzed in lncTCF7-depleted cells by quantitative real-time PCR (left penal) and western blot (right panel) analyses. Quantitative real-time PCR results are shown as means ± SD.

(C) CD13$^+$CD133$^+$ (CSC) subpopulations were detected in lncTCF7-depleted cells by FACS analysis. Results are shown as means ± SD.

(D) LncTCF7 depletion causes a diminished oncosphere-forming capacity in HCC cell lines and HCC primary cells. The right panel represents statistical results as means ± SD. Scale bar, 100 μm.

(E) Pluripotency transcripts were analyzed in lncTCF7-silenced HCC primary cells by quantitative real-time PCR analysis. Data are shown as means ± SD.

(F) LncTCF7-silenced or shCtrl HCC primary tumor cells were diluted and subcutaneously implanted into BALB/c nude mice. Tumors were observed over 4 months. n = 12 for each group.
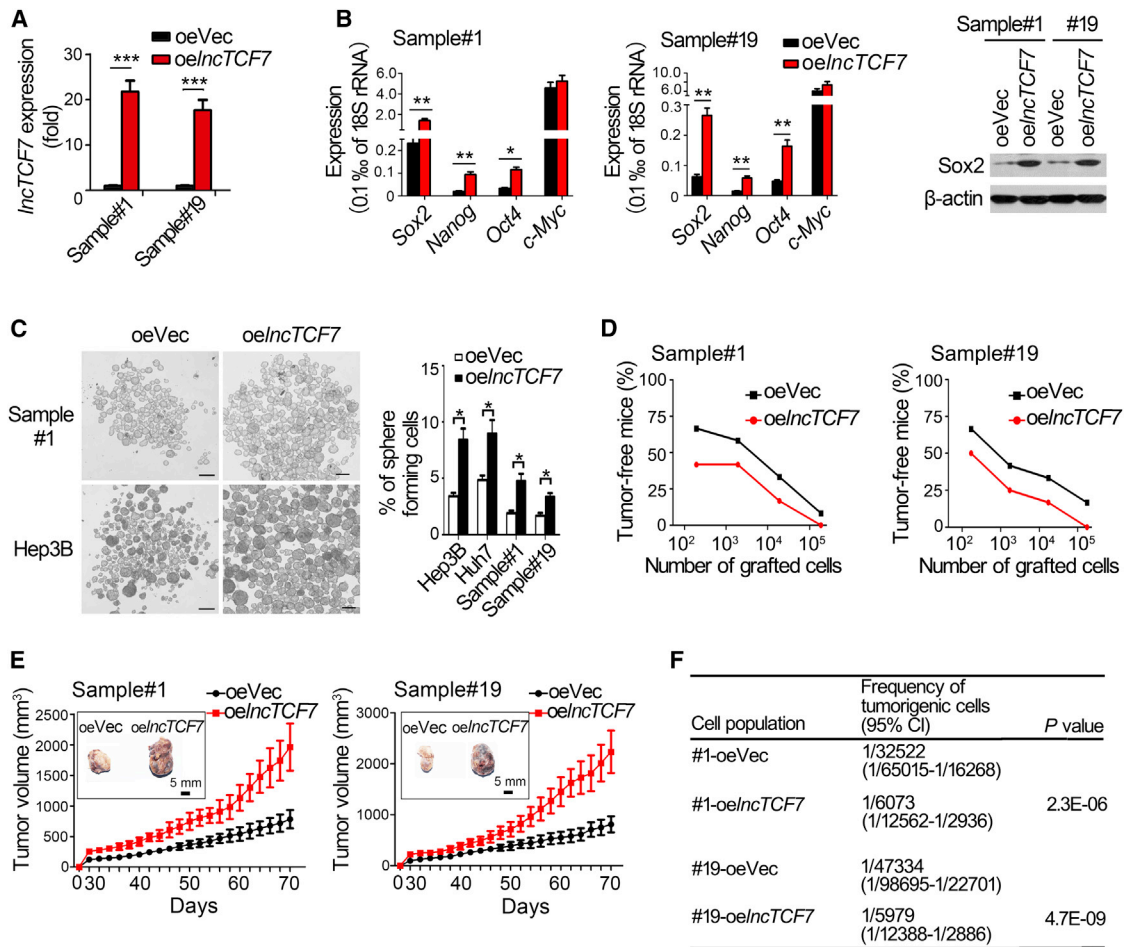
Figure 3. *LncTCF7* Overexpression Enhances Tumorigenic Capacity of Liver CSCs

(A) *LncTCF7*-overexpressing HCC primary tumor cells were established. oeVec, overexpression empty vector; oe*lncTCF7*, overexpression of *lncTCF7*. Data are shown as means ± SD.

(B) Overexpression of *lncTCF7* (oe*lncTCF7*) resulted in elevated expression of pluripotent factors in HCC cells as assessed by quantitative real-time PCR (left) and western blot (right) analyses. Quantitative real-time PCR data are shown as means ± SD.

(C) *LncTCF7* overexpression enhances the capacity of oncosphere formation. Scale bar, 100 μm. oe, overexpression. The right panel represents statistical results shown as means ± SD.

(D) *LncTCF7*-overexpressing (oe*lncTCF7*) or empty vector (oeVec) cells derived from HCC primary tumor cells were diluted and subcutaneously implanted into BALB/c nude mice. Tumors were observed over 4 months. n = 12 for each group.

(E) *LncTCF7*-overexpressing or vector control (oeVec) treated primary cells were subcutaneously injected into BALB/c nude mice for observation of tumor growth. Results are shown as means ± SD. n = 10 for each group.

(F) Tumorigenic cell frequency in *lncTCF7*-overexpressing and empty vector control (oeVec) cells was determined with limiting dilution assays (http://bioinf.wehi. edu.au/software/elda/). #1, sample #1; #19, sample #19; oe, overexpression; CI, confidence interval.

*p < 0.05, **p < 0.01, and ***p < 0.001 by two-tailed Student's t test. Data represent at least three independent experiments. See also Figure S3.

tumor growth and tumorigenic cell frequency (Figures 2G and 2H). We observed xenograft growth for 4 months and defined a threshold tumor size for detectability of tumors as 30–40 mm³. Similar observations were achieved in *lncTCF7*-silenced HCC cell lines (Figures S2F–S2H). Overall, *lncTCF7* silencing abrogates the tumorigenic capacity of liver CSCs.
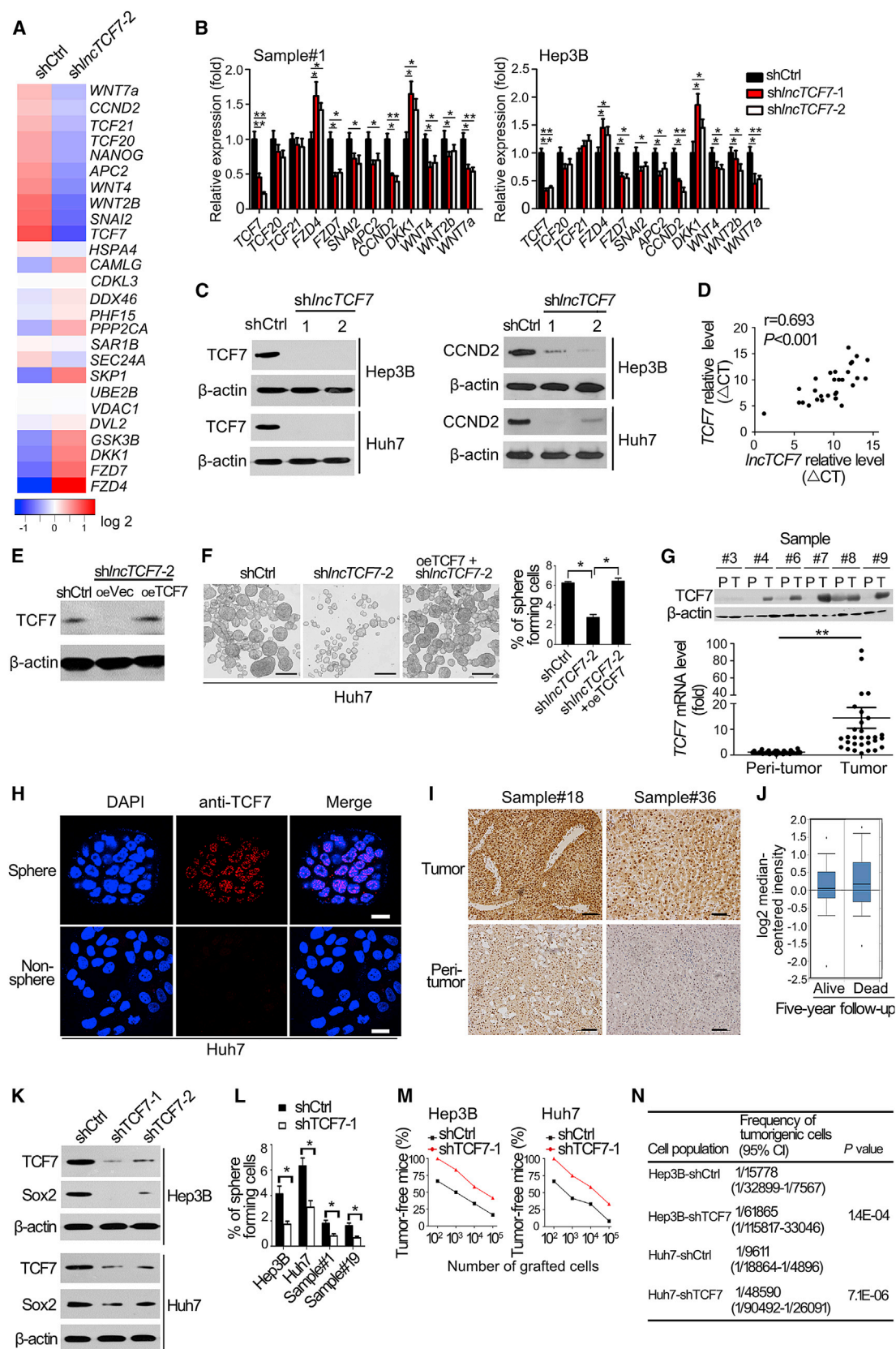
LncTCF7 Overexpression Enhances Tumorigenic Capacity of Liver CSCs

We next overexpressed *lncTCF7* in HCC primary tumor cells and cell lines and established *lncTCF7* stably overexpressing cell lines (Figure 3A and Figure S3A). *LncTCF7* overexpression dramatically increased expression of pluripotent transcription

(G) *LncTCF7*-silenced or shCtrl HCC primary tumor cells were subcutaneously injected into BALB/c nude mice for observation of tumor growth. Results are shown as means ± SD. n = 12 for each group.

(H) Tumorigenic cell frequency in *lncTCF7*-depleted and control primary tumor cells was analyzed with a limiting dilution assay (http://bioinf.wehi.edu.au/software/elda/). #1, sample #1; #19, sample #19; CI, confidence interval.

*p < 0.05, **p < 0.01, and ***p < 0.001 by two-tailed Student's t test. Data represent at least three independent experiments. See also Figure S2.

(legend on next page)

factors (Figure 3B). Notably, *lncTCF7* overexpression significantly enhanced oncosphere formation and tumor-initiating capacity (Figures 3C and 3D). Consequently, *lncTCF7* overexpression dramatically augmented xenograft tumor growth (Figure 3E) and tumorigenic cell frequency (Figure 3F). We tested at least six HCC primary samples and achieved similar observations. Similar results were also observed in *lncTCF7*-overexpressed HCC cell lines such as Hep3B and Huh7 cells (Figure S3). All together, these data indicate that *lncTCF7* plays a critical role in the self-renewal maintenance of liver CSCs.

LncTCF7 Triggers TCF7 Expression to Activate Wnt Signaling

To explore the target genes of *lncTCF7*, we established *lncTCF7*-silenced HCC primary CSC cells and conducted transcriptome microarray analysis. *LncTCF7* knockdown resulted in differential expression of 2,491 genes (Figure S4A), suggesting that *lncTCF7* regulates many genes that relate to important signaling processes including the Wnt signaling pathway (Figure S4B). Notably, *lncTCF7* knockdown significantly reduced its nearby protein-coding gene *TCF7* and some major Wnt signaling targets (Figure 4A). By contrast, *HSPA4* and the other neighboring genes displayed no significant changes. We then validated these observations in HCC cell lines (Hep3B, Huh7, and PLC) or HCC primary cells (at least six samples). Consistently, *lncTCF7* silencing remarkably reduced the expression of TCF7 and major Wnt targets in HCC cell lines and HCC primary cells we examined (Figures 4B and 4C and Figures S4C and S4D). In contrast, *lncTCF7* depletion did not alter the expression of *HSPA4* and the other neighboring genes (Figures S4C and S4E). In addition, *lncTCF7* overexpression in HCC cell lines or HCC primary cells remarkably enhanced the expression of *TCF7* and major Wnt targets (Figure S4F). These data suggest that *lncTCF7* activates the Wnt signaling pathway in HCC.

We further tested the expression levels of *lncTCF7* and *TCF7* in HCC subjects by quantitative real-time PCR. We noticed that *lncTCF7* expression was positively correlated with the expression of *TCF7* (Pearson correlation coefficient r = 0.693, p < 0.001) (Figure 4D). To determine whether *lncTCF7* functions

upstream of TCF7 in the regulation of liver CSC self-renewal, we rescued TCF7 expression in *lncTCF7*-silenced HCC cells (Figure 4E). Interestingly, TCF7 restoration rescued the oncosphere formation ability reduced by *lncTCF7* depletion (Figure 4F). Additionally, TCF7 restoration also rescued *lncTCF7*-depletion-reduced tumor-initiating capacity and xenograft tumor growth (data not shown). *LncTCF7* silencing dramatically downregulated expression of some major Wnt molecules, including Wnt7a, Wnt4, and Wnt2b (Figures 4A and 4B). Among these three Wnt molecules, *lncTCF7* depletion reduced expression of Wnt7a the most. To further validate whether Wnt7a is a downstream effector of *lncTCF7*, we incubated *lncTCF7*-silenced HCC primary CSCs with recombinant Wnt7a for a sphere formation assay. We found that Wnt7a rescued the oncosphere formation ability reduced by *lncTCF7* depletion (Figure S4G). Additionally, Wnt7a also restored the expression levels of *TCF7*, *Sox2*, and *Nanog* in *lncTCF7*-depleted HCC primary CSCs (Figure S4H). DKK1 (Dickkopf-related protein 1) was reported to be an extracellular inhibitor of Wnt signaling (Cui et al., 2013). The presence of DKK1 was able to abolish the oncosphere formation ability enabled by *lncTCF7* overexpression (Figure S4I). Consistently, DKK1 treatment also impeded the expression levels of *TCF7*, *Sox2*, and *Nanog* in *lncTCF7*-overexpressing HCC primary CSC cells (Figure S4J). These data suggest that *lncTCF7* sustains the self-renewal of liver CSCs upstream of TCF7.

To further explore the clinical implications of TCF7 in HCC, we analyzed the expression of TCF7 in HCC tumor and peri-tumor tissues. We observed that TCF7 was highly expressed in HCC tumors (Figure 4G). Additionally, TCF7 was mainly localized in the nuclei of HCC oncosphere cells, whereas it was almost undetectable in non-sphere cells (Figure 4H). High expression of TCF7 in HCC samples was further confirmed by immunohistochemistry staining (Figure 4I). Importantly, high expression of TCF7 predicted a lower rate of 5-year survival in members of a cohort analyzed by Hoshida et al. (2009) (Figure 4J). Next, we silenced TCF7 in HCC cells and established stably silenced cell lines (Figure 4K). Notably, TCF7 depletion suppressed Sox2 expression. We observed that TCF7 silencing dramatically impaired

Figure 4. *LncTCF7* Triggers TCF7 Expression to Activate Wnt Signaling in Liver CSCs
(A) Mean-centered, hierarchical clustering of genes altered in *lncTCF7*-silenced or shCtrl-treated HCC primary CSC cells.
(B) Differential genes were validated in *lncTCF7*-silenced HCC cell lines and HCC primary samples. Similar observations were obtained from three *lncTCF7*-silenced cell lines (Hep3B, Huh7, and PLC) and six HCC primary specimens we examined. Results of Hep3B and Sample#1 are represented. Data are shown as means ± SD.
(C) TCF7 and CCND2 were analyzed by immunoblotting.
(D) Expression levels of *lncTCF7* and TCF7 were detected in 30 HCC samples and subjected to correlation analysis. Data were normalized to 18S rRNA expression and shown as ΔCT (threshold cycle).
(E) TCF7 was overexpressed in *lncTCF7*-silenced Huh7 cells. oe, overexpression.
(F) TCF7 overexpression rescues sphere formation ability reduced by *lncTCF7* depletion. Representative sphere formation is shown on the left panel. Scale bar, 100 μm. Percentages of sphere-forming cells were calculated as means ± SD (right panel).
(G) TCF7 was detected in HCC tumor and peri-tumor tissues (n = 30) by western blot (upper panel) and quantitative real-time PCR (lower panel) analyses. Quantitative real-time PCR data were normalized to 18S rRNA expression and peri-tumor tissues were assigned a value of 1.
(H) TCF7 was visualized in Huh7 oncosphere and non-sphere cells by immunofluorescence staining. Scale bar, 10 μm.
(I) TCF7 was detected in HCC samples by immunohistochemistry staining. Scale bar, 100 μm.
(J) *TCF7* was analyzed in live (n = 48) and dead (n = 32) HCC subjects in accordance with the 5-year followup protocol devised in Hoshida et al. (2009) (n = 80).
(K) Sox2 was detected in TCF7-depleted or shCtrl HCC cells.
(L) *TCF7* depletion reduces the rate of oncosphere formation in cells derived from HCC cell lines and HCC primary cells. Data are shown as means ± SD.
(M and N) *TCF7* depletion reduces tumor-initiating capacity (M) and tumorigenic cell frequency (N) as analyzed by a limiting dilution assay (http://bioinf.wehi.edu.au/software/elda/). CI, confidence interval.
*p < 0.05 and **p < 0.01 by two-tailed Student's t test. Data are representative of at least three separate experiments. See also Figure S4.

oncosphere formation, tumor initiating capacity, and xenograft growth in HCC cell lines and primary cells (Figures 4L–4N, and data not shown). In sum, *lncTCF7* initiates TCF7 expression to activate the Wnt signaling pathway, leading to priming of liver CSC self-renewal and tumor propagation.

LncTCF7 Recruits the SWI/SNF Complex

LncRNAs are considered to exert their functions through RNA-interacting proteins that regulate gene expression by various mechanisms (Geisler and Coller, 2013). Therefore, we performed an RNA pull-down assay with biotin-labeled *lncTCF7* to search for potential *lncTCF7*-associated proteins. BRG1, BAF170, and SNF5, three core subunits of the SWI/SNF complex, were identified to bind *lncTCF7* in liver CSCs (Figures 5A and 5B and Figures S5A–S5C). The interaction of *lncTCF7* with the three SWI/SNF components was further validated by RNA immunoprecipitation (RIP) (Figure 5C and Figure S5D). However, *lncTCF7* depletion did not influence expression levels of BAF170, BRG1, and SNF5 (Figure 5D), suggesting that *lncTCF7* was not involved in the post-translational regulation of the SWI/SNF complex. Moreover, *lncTCF7* colocalized with BAF170 in the nuclei of HCC oncosphere cells, whereas *lncTCF7* was poorly expressed in the nuclei of non-sphere cells (Figure 5E). These data indicate that *lncTCF7* associates with the SWI/SNF complex in the nuclei of liver CSCs.

We next constructed a series of *lncTCF7* truncations to map its binding fragment with the SWI/SNF complex. We found that the 3′-end fragment of *lncTCF7* (nt 468 to 683) was sufficient to bind BAF170, BRG1, and SNF5 (Figure 5F). A stable stem-loop structure of the 3′-end fragment was predicted by RNA folding analysis (Figure S5E). The binding of the 3′-end region of *lncTCF7* with BAF170 was further confirmed by an RNA electrical mobility shift assay (EMSA) (Figures 5G and 5H). Unlabeled *lncTCF7* probes competitively disrupted this binding capacity. Additionally, *lncTCF7* showed high binding affinity (dissociation constant [Kd] 36.24 nM) (Figure 5I). These data indicate that *lncTCF7* directly binds to the SWI/SNF complex with high affinity.

LncTCF7 Triggers TCF7 Expression to Activate Wnt Signaling

Given that the SWI/SNF complex regulates gene transcription by binding to promoter loci and refolding chromatin (Roberts and Orkin, 2004), we then detected whether *lncTCF7* influenced BAF170 occupancy of the promoter locus of the *TCF7* gene. We analyzed a 3 kb locus upstream from the transcription start sites (TSSs) of the *TCF7* gene. We found that *lncTCF7* depletion abrogated the binding capacity of BAF170 with (approximately) a −1,160 to −1,048 bp segment of *TCF7* promoter (Figure 6A), suggesting that this segment was the binding site for *lncTCF7*. Through luciferase reporter assays, we identified (approximately) a −1,200 to −1,100 bp segment of *TCF7* promoter as a sufficient binding site for BAF170 (Figures 6B–6D). Finally, we observed via a DNase I digestion assay that *lncTCF7* or BAF170 knockdown significantly impaired the chromatin accessibility of the *TCF7* locus (Figure 4E). By contrast, BAF170 was not recruited on the promoters of the stem pluripotent factors, as assessed through chromatin immunoprecipitation (ChIP) analyses (Figures S6A–S6D), suggesting that BAF170 had an indirect effect on the expression of stem pluripotent factors. These

data suggest that *lncTCF7* recruits the SWI/SNF complex to the *TCF7* promoter, thereby leading to its activation.

Notably, the SWI/SNF complex was highly expressed in HCC tumors and liver CSCs (Figure 6F and data not shown), suggesting that the SWI/SNF complex may be implicated in the regulation of liver CSC self-renewal. Consequently, BAF170 depletion dramatically reduced expression of TCF7 and Nanog (Figure 6G), as well as Wnt downstream targets such as Sox2, CCND1, and CCND2. Additionally, BAF170 knockdown significantly impaired the ability of oncosphere formation derived from HCC cell lines and HCC primary cells (Figure 6H). Finally, BAF170 knockdown also remarkably reduced tumor-initiating capacity and xenograft tumor growth (Figures 6I–6K). Similar results were observed by depleting SNF5 and BRG1 (data not shown). All together, our data show that *lncTCF7* triggers TCF7 expression through recruitment of the SWI/SNF complex, leading to priming of the self-renewal of liver CSCs and tumor initiation.

DISCUSSION

Recently, CSCs have been identified in many solid tumors, including breast, lung, liver, brain, colon, prostate, and bladder cancers (Haraguchi et al., 2010; O'Brien et al., 2007; Visvader and Lindeman, 2012). CSCs have stem characteristics such as self-renewal and differentiation. CSCs may account for cancer relapse and metastasis due to their invasive and drug-resistant capacities (Gupta et al., 2009). Several surface markers have been identified in liver CSCs. However, details of liver CSC biology remain largely unknown. In this study, we isolated the CD13$^+$CD133$^+$ subpopulation of cells from HCC cell lines and HCC primary cells and identified them as liver CSCs. Through transcriptome microarray analysis, we identified 286 differentially expressed noncoding RNAs in liver CSCs. Among these highly expressed lncRNAs in liver CSCs, we defined an lncRNA termed *lncTCF7* that plays a critical role in priming the self-renewal of liver CSCs.

LncRNAs have been reported to play widespread roles in gene regulation and other cellular processes (Batista and Chang, 2013; Flynn and Chang, 2014). LncRNAs exert their functions via diverse mechanisms, including cotranscriptional regulation, modulation of gene expression, scaffolding of nuclear or cytoplasmic complexes, and pairing with other RNAs (Ulitsky and Bartel, 2013). Notably, accumulating evidence shows that lncRNAs modulate gene expression as epigenetic modifiers (Kaneko et al., 2014; Klattenhoff et al., 2013; Prensner et al., 2013; Tsai et al., 2010; Zhu et al., 2013). Here we found that *lncTCF7* activates TCF7 expression in *cis* through recruitment of the SWI/SNF complex. TCF7 expression triggers Wnt signaling to initiate self-renewal of liver CSCs. Although *lncTCF7* is expressed in the antisense direction, it fails to form an *lncTCF7*-TCF7 mRNA complex for the regulation of TCF7 expression. The Wnt signaling plays a pivotal role in self-renewal and differentiation of CSCs (Hoffmeyer et al., 2012; Myant et al., 2013). Aberrant activation of Wnt signaling is implicated in liver cancer and other chronic liver diseases (Huch et al., 2013; Wang et al., 2013a). Here we show that depletion of TCF7 and Wnt downstream target genes impairs the self-renewal of liver CSCs and their tumor-initiating capacity, suggesting that TCF7-mediated
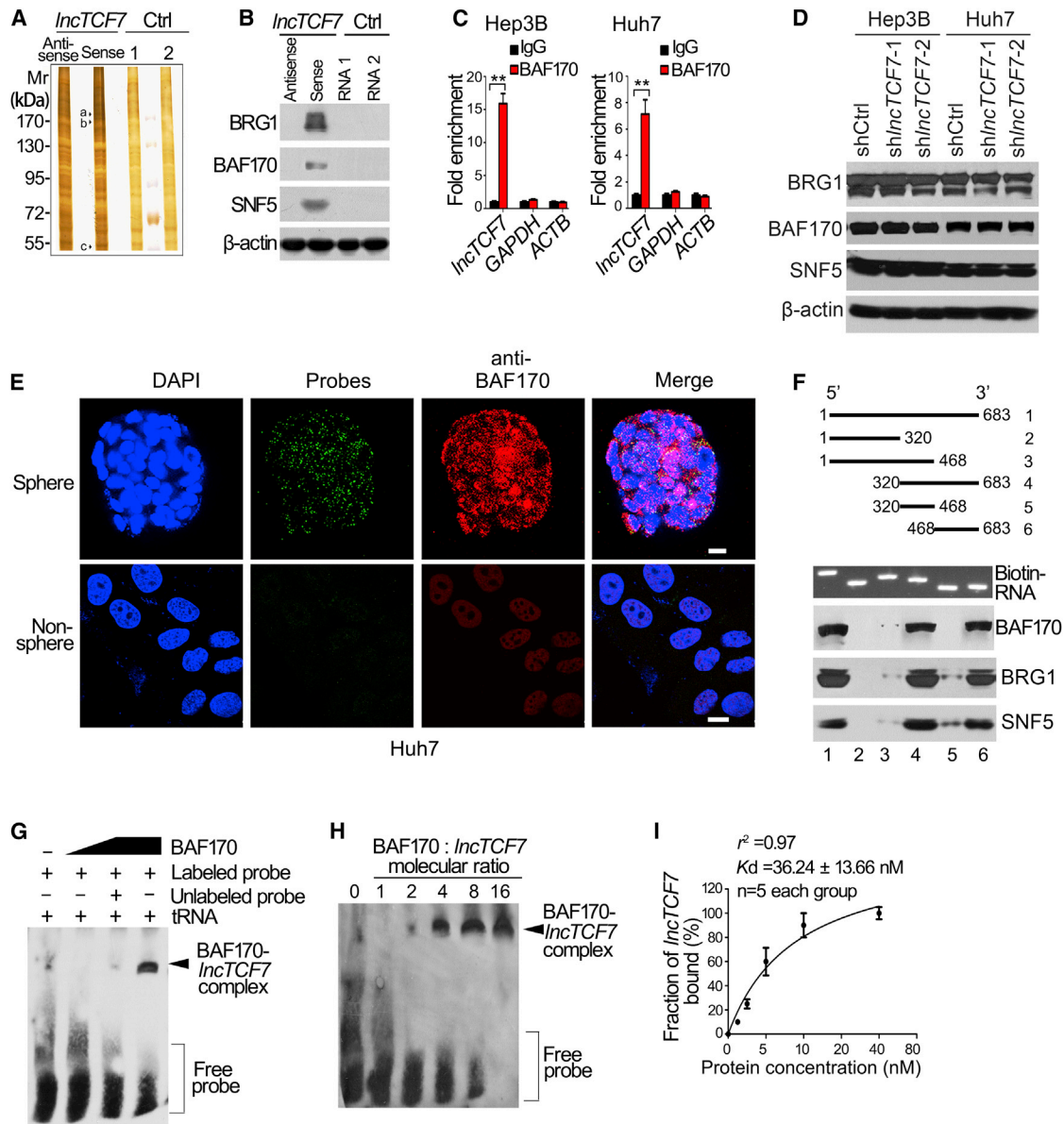
Figure 5. *LncTCF7* Associates with the SWI/SNF Complex

(A) Biotin-RNA pull-downs were performed with nuclear extracts of oncosphere cells using full-length *lncTCF7* transcript (sense), antisense, and other two *lncTCF7* intron controls. This was followed by mass spectrometry. Band a, BRG1; band b, BAF170; band c, SNF5.

(B) Three core components of the SWI/SNF complex were confirmed by immunoblotting. β-actin was used as a loading control.

(C) The interaction of *lncTCF7* with BAF170, BRG1, and SNF5 was verified by an RNA immunoprecipitation (RIP) assay. Results are shown as means ± SD. **p < 0.01 by two-tailed Student's t test.

(D) *LncTCF7* depletion does not alter the protein levels of BAF170, BRG1, and SNF5.

(E) *LncTCF7* was visualized by RNA-FISH, and immunofluorescence staining of BAF170 in Huh7 oncosphere and non-sphere cells was performed. Scale bar, 10 μm.

(F) Mapping analysis of SWI/SNF-complex-binding domains of *lncTCF7*. Shown are the following: schematic diagram of *lncTCF7* full-length and truncated fragments (top panel); in vitro transcribed biotin-labeled RNA (middle panel); and western blot of BAF170, BRG1, and SNF5 in RNA pull-down samples by different *lncTCF7* fragments (bottom panel).

(G) BAF170 protein and biotin-labeled *lncTCF7* (468-683 nt) probes were incubated for an EMSA assay.

(H) Different concentrations of BAF170 protein were incubated with *lncTCF7* probes (5 nM) and followed by EMSA assays as above (G).

(I) Binding affinity of *lncTCF7* with BAF170 as determined by five independent EMSA assays. Non-linear regression curves were generated by GraphPad Prism. See also Figure S5.
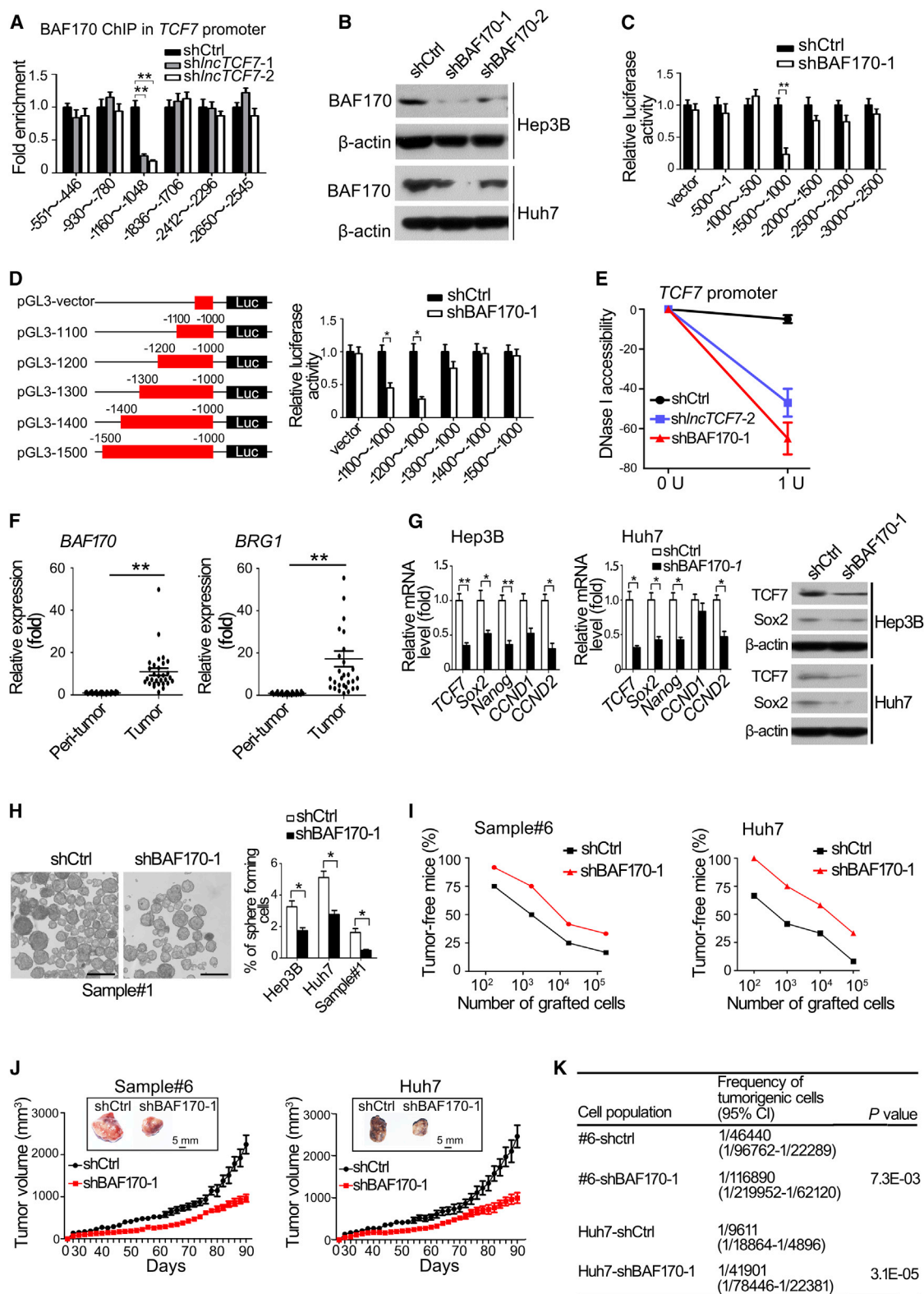
Figure 6. *LncTCF7* Triggers TCF7 Expression to Activate Wnt Signaling
(A) An approximately 1,160–1,048 bp fragment of the *TCF7* promoter is sufficient for the binding of BAF170 by ChIP-quantitative PCR analysis. Data are shown as means ± SD.
(B) BAF170 was silenced in liver CSCs by two independent shRNAs.

Wnt signaling is critical for sustaining liver CSC self-renewal and tumorigenicity.

CSCs harbor the stem cell properties of self-renewal and differentiation (Visvader and Lindeman, 2012). In this study, we found that there was no significant difference in the proliferative capacity between liver CSCs and non-CSCs, as assessed by cell-cycle analysis and immunofluorescence staining. Actually, CSCs exist mainly in the G1/G0 phase or G0 phase with dormant or slow-growing properties (Haraguchi et al., 2010). As such, it might be hard to distinguish the proliferation differences between liver CSCs and non-CSCs via Ki67 staining or DNA contents assayed by propidium iodide (PI). Also, the self-renewal properties of different cancer types may have different proliferation characteristics. The maintenance of self-renewal is an extremely complicated biological process, which is controlled by epigenetic states, pluripotent transcription factors, epigenetic complexes, and many developmental pathways (Boumahdi et al., 2014; Ohnishi et al., 2014; Visvader and Lindeman, 2012). Our data support the idea that *lncTCF7*-mediated Wnt signaling activation in hepatic CSCs plays a critical role in the regulation of liver CSC self-renewal.

TCF7, as a T cell factor, is best known for its function in T lymphocyte development and multipotential hematopoietic cell self-renewal (Weber et al., 2011). TCF7 can initiate the Wnt signaling cascade as an upstream trigger (Cui et al., 2013; Weber et al., 2011). $TCF7^{-/-}$ mice developed intestinal and mammary adenomas, implying a role for TCF7 in tumor suppression (Yu et al., 2012). In this study, we demonstrate that TCF7 is required for the self-renewal of liver CSCs and tumor propagation and acts as a tumor promoter. TCF7 is regulated by *lncTCF7* in liver CSCs to trigger the Wnt signaling pathway, which primes the self-renewal of liver CSCs. A recent study reported that TCF7 functions as a tumor enhancer in tumorigenesis after ocular transplantation of embryonic stem cell-derived retinal progenitor cells (Cui et al., 2013). Consistently, our findings reveal that *lncTCF7* mediated TCF7 expression, which initiates the Wnt signaling cascade to prime self-renewal of liver CSCs and hepatic tumorigenicity as a tumor promoter. CSCs are analogous to tissue-specific stem cells in that they contribute to long-term growth and are responsible for the maintenance and growth of tumors (Beck and Blanpain, 2013). Transcriptional regulation is one of the key regulatory mechanisms determining cell fate, which includes *cis*-regulatory elements and transacting factors. Among all transacting factors, chromatin remodeling regulation plays a pivotal role in gene transcription (Krasteva et al., 2012; Narlikar et al., 2013), which depends on ATP-dependent chromatin remodeling complexes. The SWI/SNF complex is composed of 12–15 subunits containing one of the two catalytic ATPase subunits, SMARCA4/BRG1 or SMARCA2/BRM, and several core components such as SMARCB1/SNF5, BAF170, and BAF155 (Helming et al., 2014; Wilson and Roberts, 2011). The SWI/SNF complex regulates gene expression through mobilizing nucleosomes and remodeling chromatin using the energy of ATP hydrolysis, suggesting its critical role in gene expression. Inactivating mutations in several SWI/SNF subunits cause various human cancers (Helming et al., 2014; Jones et al., 2010; Kadoch et al., 2013), suggesting that some components act as tumor suppressors. A recent study reported that the long noncoding RNA *SChLAP1* associates with the SNF5 subunit to promote prostate cancer progress by antagonizing the function of the SWI/SNF complex (Prensner et al., 2013), which implies that SNF5 functions as a tumor suppressor. Here we found that *lncTCF7* can recruit the SWI/SNF complex to trigger TCF7 expression, leading to priming of liver CSC self-renewal. Additionally, we observed that BAF170, BRG1, and SNF5 are highly expressed in HCC specimens and liver CSCs, whose depletion impairs tumor-initiating capacity and tumor propagation (Figure 6, and data not shown), suggesting that these three components act as tumor promoters. Therefore, how the SWI/SNF complex components function in tumorigenesis remains to be further investigated.

In conclusion, *lncTCF7* can promote liver CSC self-renewal and tumor propagation through activation of Wnt signaling by recruiting the SWI/SNF complex to the *TCF7* promoter. Our findings reveal that lncRNAs may represent an additional layer of regulation of oncogenesis.

EXPERIMENTAL PROCEDURES

Northern Blot Analysis

Total RNA, extracted as described (Wang et al., 2013b) from human CSC oncospheres and control cells, was subjected to northern blot assays. An *lncTCF7*-specific DNA sequence (nt320–683) was cloned into pcDNA4/*myc*-his B Vector. Radioactive RNA probe with a length of 363 nt was generated using [α-^{32}P] CTP (Perkin Elmer) and the Riboprobe in vitro transcription labeling system (Promega).

(C and D) Different loci of TCF7 promoter were constructed into pGL3 vector and subjected to luciferase reporter assays in BAF170-silenced cells. Data are shown as means ± SD.

(E) LncTCF7 or BAF170 depletion increases chromatin accessibility at the promoter of TCF7 by DNase I digestion assays. Data are shown as means ± SD.

(F) *BAF170* and *BRG1* were highly expressed in HCC tumor tissues (n = 30). Data were normalized to endogenous 18S rRNA expression and peri-tumor tissues were assigned a value of 1.

(G) TCF7, pluripotent transcripts, and Wnt pathway targets were detected in BAF170-silenced HCC cells by quantitative real-time PCR (left panel) and western blot (right panel) analyses. Quantitative PCR data are shown as means ± SD.

(H) BAF170 depletion impairs the capacity of oncosphere formation in cells derived from HCC cell lines and HCC primary cells. Scale bar, 100 μm. Percentages of sphere-forming cells were calculated as means ± SD (right panel).

(I) BAF170-silenced or shCtrl HCC primary tumor cells or Huh7 cells were diluted and subcutaneously implanted into BALB/c nude mice. Tumors were observed during 4 months. n = 6 for each group.

(J) BAF170-silenced or shCtrl HCC primary tumor cells and Huh7 cells were subcutaneously injected into BALB/c nude mice for observation of tumor growth. Results are shown as means ± SD. n = 10 for each group.

(K) Tumorigenic cell frequency in BAF170-silenced and shCtrl primary tumor cells was analyzed with a limiting dilution assay (http://bioinf.wehi.edu.au/software/elda/). #6, sample #6; CI, confidence interval.

*p < 0.05 and **p < 0.01 by two-tailed Student's t test. Data represent at least three independent experiments. See also Figure S6.

RNA-FISH

Fluorescence-conjugated *lncTCF7* probes were used for RNA-FISH. RNA-FISH was performed as previously described (Wang et al., 2014). Hybridization was carried out using DNA probe sets (Biosearch Technologies) according to the protocol of Biosearch Technologies. Oncosphere and control cells were observed with a FV1000 confocal laser microscope (Olympus).

RNA Pull-down and Mass Spectrometry Assay

RNA pull-down was performed as described (Klattenhoff et al., 2013). In vitro biotin-labeled RNAs (*lncTCF7*, its antisense RNA, and two control RNAs from two introns of *lncTCF7*) were transcribed with the biotin RNA labeling mix (Roche) and T7 RNA polymerase (Roche) treated with RNase-free DNase I (Promega) and purified with RNeasy Mini Kit (QIAGEN). Biotinylated RNA was incubated with HCC oncosphere cell nuclear extracts, and pull-down proteins were run on SDS-PAGE gels as described (Xia et al., 2013). Mass spectrometry followed.

RNA-EMSA Assay

EMSA experiments were performed using a LightShift Chemiluminescent RNA EMSA Kit (Thermo Scientific). The shifted signals were quantified and plotted against the amount of BAF170 protein with GraphPad Prism 6 (GraphPad).

Statistical Analysis

Data were analyzed with a double-sided Student's t test using the SPSS 13.0 software and GraphPad Prism 6. Tumorigenic cell frequency was calculated based on extreme limiting dilution analysis (ELDA) (http://bioinf.wehi.edu.au/software/elda/). $p < 0.05$ was considered statistically significant. For other methods see the Supplemental Information.

ACCESSION NUMBERS

Microarray data have been deposited in the NCBI GEO under accession numbers GSE66515 and GSE66529.

SUPPLEMENTAL INFORMATION

Supplemental Information for this article includes six figures, one table, and Supplemental Experimental Procedures and can be found with this article online at http://dx.doi.org/10.1016/j.stem.2015.03.003.

AUTHOR CONTRIBUTIONS

Y.W. designed and performed experiments, analyzed data, and wrote the paper, and L.H. provided clinical specimens and analyzed data. P.Z., G.H., and J.L. constructed plasmids and analyzed data; Y.D., X.Y., C.L., P.X., and G.Z. performed some experiments; B.Y. and Y.T. performed some experiments and analyzed data; R.C. initiated the study; and Z.F. initiated the study and organized, designed, and wrote the paper.

REFERENCES

Batista, P.J., and Chang, H.Y. (2013). Long noncoding RNAs: cellular address codes in development and disease. Cell *152*, 1298–1307.

Beck, B., and Blanpain, C. (2013). Unravelling cancer stem cell potential. Nat. Rev. Cancer *13*, 727–738.

Boumahdi, S., Driessens, G., Lapouge, G., Rorive, S., Nassar, D., Le Mercier, M., Delatte, B., Caauwe, A., Lenglez, S., Nkusi, E., et al. (2014). SOX2 controls tumour initiation and cancer stem-cell functions in squamous-cell carcinoma. Nature *511*, 246–250.

Cech, T.R., and Steitz, J.A. (2014). The noncoding RNA revolution-trashing old rules to forge new ones. Cell *157*, 77–94.

Cui, L., Guan, Y., Qu, Z., Zhang, J., Liao, B., Ma, B., Qian, J., Li, D., Li, W., Xu, G.T., and Jin, Y. (2013). WNT signaling determines tumorigenicity and function of ESC-derived retinal progenitors. J. Clin. Invest. *123*, 1647–1661.

Easwaran, H., Tsai, H.C., and Baylin, S.B. (2014). Cancer epigenetics: tumor heterogeneity, plasticity of stem-like states, and drug resistance. Mol. Cell *54*, 716–727.

Eroglu, E., Burkard, T.R., Jiang, Y., Saini, N., Homem, C.C., Reichert, H., and Knoblich, J.A. (2014). SWI/SNF complex prevents lineage reversion and induces temporal patterning in neural stem cells. Cell *156*, 1259–1273.

Flynn, R.A., and Chang, H.Y. (2014). Long noncoding RNAs in cell-fate programming and reprogramming. Cell Stem Cell *14*, 752–761.

Geisler, S., and Coller, J. (2013). RNA in unexpected places: long non-coding RNA functions in diverse cellular contexts. Nat. Rev. Mol. Cell Biol. *14*, 699–712.

Gupta, P.B., Chaffer, C.L., and Weinberg, R.A. (2009). Cancer stem cells: mirage or reality? Nat. Med. *15*, 1010–1012.

Gupta, R.A., Shah, N., Wang, K.C., Kim, J., Horlings, H.M., Wong, D.J., Tsai, M.C., Hung, T., Argani, P., Rinn, J.L., et al. (2010). Long non-coding RNA HOTAIR reprograms chromatin state to promote cancer metastasis. Nature *464*, 1071–1076.

Haraguchi, N., Ishii, H., Mimori, K., Tanaka, F., Ohkuma, M., Kim, H.M., Akita, H., Takiuchi, D., Hatano, H., Nagano, H., et al. (2010). CD13 is a therapeutic target in human liver cancer stem cells. J. Clin. Invest. *120*, 3326–3339.

Helming, K.C., Wang, X., and Roberts, C.W. (2014). Vulnerabilities of mutant SWI/SNF complexes in cancer. Cancer Cell *26*, 309–317.

Hoffmeyer, K., Raggioli, A., Rudloff, S., Anton, R., Hierholzer, A., Del Valle, I., Hein, K., Vogt, R., and Kemler, R. (2012). Wnt/β-catenin signaling regulates telomerase in stem cells and cancer cells. Science *336*, 1549–1554.

Hoshida, Y., Nijman, S.M., Kobayashi, M., Chan, J.A., Brunet, J.P., Chiang, D.Y., Villanueva, A., Newell, P., Ikeda, K., Hashimoto, M., et al. (2009). Integrative transcriptome analysis reveals common molecular subclasses of human hepatocellular carcinoma. Cancer Res. *69*, 7385–7392.

Huch, M., Dorrell, C., Boj, S.F., van Es, J.H., Li, V.S., van de Wetering, M., Sato, T., Hamer, K., Sasaki, N., Finegold, M.J., et al. (2013). In vitro expansion of single Lgr5+ liver stem cells induced by Wnt-driven regeneration. Nature *494*, 247–250.

Jemal, A., Bray, F., Center, M.M., Ferlay, J., Ward, E., and Forman, D. (2011). Global cancer statistics. CA Cancer J. Clin. *61*, 69–90.

Ji, J., Shi, J., Budhu, A., Yu, Z., Forgues, M., Roessler, S., Ambs, S., Chen, Y., Meltzer, P.S., Croce, C.M., et al. (2009). MicroRNA expression, survival, and response to interferon in liver cancer. N. Engl. J. Med. *361*, 1437–1447.

Jones, S., Wang, T.L., Shih, IeM., Mao, T.L., Nakayama, K., Roden, R., Glas, R., Slamon, D., Diaz, L.A., Jr., Vogelstein, B., et al. (2010). Frequent mutations of chromatin remodeling gene ARID1A in ovarian clear cell carcinoma. Science *330*, 228–231.

Kadoch, C., Hargreaves, D.C., Hodges, C., Elias, L., Ho, L., Ranish, J., and Crabtree, G.R. (2013). Proteomic and bioinformatic analysis of mammalian SWI/SNF complexes identifies extensive roles in human malignancy. Nat. Genet. *45*, 592–601.

Kaneko, S., Bonasio, R., Saldaña-Meyer, R., Yoshida, T., Son, J., Nishino, K., Umezawa, A., and Reinberg, D. (2014). Interactions between JARID2 and non-coding RNAs regulate PRC2 recruitment to chromatin. Mol. Cell *53*, 290–300.

Klattenhoff, C.A., Scheuermann, J.C., Surface, L.E., Bradley, R.K., Fields, P.A., Steinhauser, M.L., Ding, H., Butty, V.L., Torrey, L., Haas, S., et al. (2013). Braveheart, a long noncoding RNA required for cardiovascular lineage commitment. Cell *152*, 570–583.

Krasteva, V., Buscarlet, M., Diaz-Tellez, A., Bernard, M.A., Crabtree, G.R., and Lessard, J.A. (2012). The BAF53a subunit of SWI/SNF-like BAF complexes is essential for hemopoietic stem cell function. Blood *120*, 4720–4732.

Lee, T.K., Castilho, A., Cheung, V.C., Tang, K.H., Ma, S., and Ng, I.O. (2011). CD24(+) liver tumor-initiating cells drive self-renewal and tumor initiation through STAT3-mediated NANOG regulation. Cell Stem Cell *9*, 50–63.

Li, M., Zhao, H., Zhang, X., Wood, L.D., Anders, R.A., Choti, M.A., Pawlik, T.M., Daniel, H.D., Kannangai, R., Offerhaus, G.J., et al. (2011). Inactivating mutations of the chromatin remodeling gene ARID2 in hepatocellular carcinoma. Nat. Genet. *43*, 828–829.

Ma, S., Chan, K.W., Hu, L., Lee, T.K., Wo, J.Y., Ng, I.O., Zheng, B.J., and Guan, X.Y. (2007). Identification and characterization of tumorigenic liver cancer stem/progenitor cells. Gastroenterology *132*, 2542–2556.

Myant, K.B., Cammareri, P., McGhee, E.J., Ridgway, R.A., Huels, D.J., Cordero, J.B., Schwitalla, S., Kalna, G., Ogg, E.L., Athineos, D., et al. (2013). ROS production and NF-κB activation triggered by RAC1 facilitate WNT-driven intestinal stem cell proliferation and colorectal cancer initiation. Cell Stem Cell *12*, 761–773.

Narlikar, G.J., Sundaramoorthy, R., and Owen-Hughes, T. (2013). Mechanisms and functions of ATP-dependent chromatin-remodeling enzymes. Cell *154*, 490–503.

O'Brien, C.A., Pollett, A., Gallinger, S., and Dick, J.E. (2007). A human colon cancer cell capable of initiating tumour growth in immunodeficient mice. Nature *445*, 106–110.

Ohnishi, K., Semi, K., Yamamoto, T., Shimizu, M., Tanaka, A., Mitsunaga, K., Okita, K., Osafune, K., Arioka, Y., Maeda, T., et al. (2014). Premature termination of reprogramming in vivo leads to cancer development through altered epigenetic regulation. Cell *156*, 663–677.

Prensner, J.R., Iyer, M.K., Sahu, A., Asangani, I.A., Cao, Q., Patel, L., Vergara, I.A., Davicioni, E., Erho, N., Ghadessi, M., et al. (2013). The long noncoding RNA SChLAP1 promotes aggressive prostate cancer and antagonizes the SWI/SNF complex. Nat. Genet. *45*, 1392–1398.

Rinn, J.L., and Chang, H.Y. (2012). Genome regulation by long noncoding RNAs. Annu. Rev. Biochem. *81*, 145–166.

Roberts, C.W., and Orkin, S.H. (2004). The SWI/SNF complex—chromatin and cancer. Nat. Rev. Cancer *4*, 133–142.

Tolstorukov, M.Y., Sansam, C.G., Lu, P., Koellhoffer, E.C., Helming, K.C., Alver, B.H., Tillman, E.J., Evans, J.A., Wilson, B.G., Park, P.J., and Roberts, C.W. (2013). Swi/Snf chromatin remodeling/tumor suppressor complex establishes nucleosome occupancy at target promoters. Proc. Natl. Acad. Sci. USA *110*, 10165–10170.

Tsai, M.C., Manor, O., Wan, Y., Mosammaparast, N., Wang, J.K., Lan, F., Shi, Y., Segal, E., and Chang, H.Y. (2010). Long noncoding RNA as modular scaffold of histone modification complexes. Science *329*, 689–693.

Ulitsky, I., and Bartel, D.P. (2013). lincRNAs: genomics, evolution, and mechanisms. Cell *154*, 26–46.

Visvader, J.E. (2011). Cells of origin in cancer. Nature *469*, 314–322.

Visvader, J.E., and Lindeman, G.J. (2012). Cancer stem cells: current status and evolving complexities. Cell Stem Cell *10*, 717–728.

Wang, J., Park, J.S., Wei, Y., Rajurkar, M., Cotton, J.L., Fan, Q., Lewis, B.C., Ji, H., and Mao, J. (2013a). TRIB2 acts downstream of Wnt/TCF in liver cancer cells to regulate YAP and C/EBPα function. Mol. Cell *51*, 211–225.

Wang, S., Xia, P., Ye, B., Huang, G., Liu, J., and Fan, Z. (2013b). Transient activation of autophagy via Sox2-mediated suppression of mTOR is an important early step in reprogramming to pluripotency. Cell Stem Cell *13*, 617–625.

Wang, P., Xue, Y., Han, Y., Lin, L., Wu, C., Xu, S., Jiang, Z., Xu, J., Liu, Q., and Cao, X. (2014). The STAT3-binding long noncoding RNA lnc-DC controls human dendritic cell differentiation. Science *344*, 310–313.

Weber, B.N., Chi, A.W., Chavez, A., Yashiro-Ohtani, Y., Yang, Q., Shestova, O., and Bhandoola, A. (2011). A critical role for TCF-1 in T-lineage specification and differentiation. Nature *476*, 63–68.

Wilson, B.G., and Roberts, C.W. (2011). SWI/SNF nucleosome remodellers and cancer. Nat. Rev. Cancer *11*, 481–492.

Xia, P., Wang, S., Du, Y., Zhao, Z., Shi, L., Sun, L., Huang, G., Ye, B., Li, C., Dai, Z., et al. (2013). WASH inhibits autophagy through suppression of Beclin 1 ubiquitination. EMBO J. *32*, 2685–2696.

Yamashita, T., and Wang, X.W. (2013). Cancer stem cells in the development of liver cancer. J. Clin. Invest. *123*, 1911–1918.

Yang, F., Huo, X.S., Yuan, S.X., Zhang, L., Zhou, W.P., Wang, F., and Sun, S.H. (2013). Repression of the long noncoding RNA-LET by histone deacetylase 3 contributes to hypoxia-mediated metastasis. Mol. Cell *49*, 1083–1096.

You, J.S., De Carvalho, D.D., Dai, C., Liu, M., Pandiyan, K., Zhou, X.J., Liang, G., and Jones, P.A. (2013). SNF5 is an essential executor of epigenetic regulation during differentiation. PLoS Genet. *9*, e1003459.

Yu, S., Zhou, X., Steinke, F.C., Liu, C., Chen, S.C., Zagorodna, O., Jing, X., Yokota, Y., Meyerholz, D.K., Mullighan, C.G., et al. (2012). The TCF-1 and LEF-1 transcription factors have cooperative and opposing roles in T cell development and malignancy. Immunity *37*, 813–826.

Yu, Y., Chen, Y., Kim, B., Wang, H., Zhao, C., He, X., Liu, L., Liu, W., Wu, L.M., Mao, M., et al. (2013). Olig2 targets chromatin remodelers to enhancers to initiate oligodendrocyte differentiation. Cell *152*, 248–261.

Yuan, J.H., Yang, F., Wang, F., Ma, J.Z., Guo, Y.J., Tao, Q.F., Liu, F., Pan, W., Wang, T.T., Zhou, C.C., et al. (2014). A long noncoding RNA activated by TGF-β promotes the invasion-metastasis cascade in hepatocellular carcinoma. Cancer Cell *25*, 666–681.

Zeng, X., Lin, X., and Hou, S.X. (2013). The Osa-containing SWI/SNF chromatin-remodeling complex regulates stem cell commitment in the adult Drosophila intestine. Development *140*, 3532–3540.

Zhao, W., Wang, L., Han, H., Jin, K., Lin, N., Guo, T., Chen, Y., Cheng, H., Lu, F., Fang, W., et al. (2013). 1B50-1, a mAb raised against recurrent tumor cells, targets liver tumor-initiating cells by binding to the calcium channel α2δ1 subunit. Cancer Cell *23*, 541–556.

Zhu, Y., Rowley, M.J., Böhmdorfer, G., and Wierzbicki, A.T. (2013). A SWI/SNF chromatin-remodeling complex acts in noncoding RNA-mediated transcriptional silencing. Mol. Cell *49*, 298–309.